



Universiteit
Leiden
The Netherlands

Phosphorylation of conserved PIN motifs directs *Arabidopsis* PIN1 polarity and auxin transport.

Huang, F.; Kemel Zago, M.; Abas, L.; Marion, A. van; Galvan-Ampudia, C.S.; Offringa, R.

Citation

Huang, F., Kemel Zago, M., Abas, L., Marion, A. van, Galvan-Ampudia, C. S., & Offringa, R. (2010). Phosphorylation of conserved PIN motifs directs *Arabidopsis* PIN1 polarity and auxin transport. *Plant Cell*, 22, 1129-1142. doi:10.1105/tpc.109.072678

Version: Not Applicable (or Unknown)

License: [Leiden University Non-exclusive license](#)

Downloaded from: <https://hdl.handle.net/1887/61849>

Note: To cite this publication please use the final published version (if applicable).

Phosphorylation of Conserved PIN Motifs Directs *Arabidopsis* PIN1 Polarity and Auxin Transport^{W OA}

Fang Huang,^a Marcelo Kemel Zago,^{a,1} Lindy Abas,^b Arnoud van Marion,^a Carlos Samuel Galván-Ampudia,^{a,2} and Remko Offringa^{a,3}

^a Department of Molecular and Developmental Genetics, Institute of Biology, Leiden University, 2333 EB Leiden, The Netherlands

^b Institute for Applied Genetics and Cell Biology, University of Natural Resources and Applied Life Sciences (BOKU Wien), A-1190 Vienna, Austria

Polar cell-to-cell transport of auxin by plasma membrane–localized PIN-FORMED (PIN) auxin efflux carriers generates auxin gradients that provide positional information for various plant developmental processes. The apical-basal polar localization of the PIN proteins that determines the direction of auxin flow is controlled by reversible phosphorylation of the PIN hydrophilic loop (PINHL). Here, we identified three evolutionarily conserved TPRXS(N/S) motifs within the PIN1HL and proved that the central Ser residues were phosphorylated by the PINOID (PID) kinase. Loss-of-phosphorylation PIN1:green fluorescent protein (GFP) (Ser to Ala) induced inflorescence defects, correlating with their basal localization in the shoot apex, and induced internalization of PIN1:GFP during embryogenesis, leading to strong embryo defects. Conversely, phosphomimic PIN1:GFP (Ser to Glu) showed apical localization in the shoot apex but did not rescue *pin1* inflorescence defects. Both loss-of-phosphorylation and phosphomimic PIN1:GFP proteins were insensitive to *PID* overexpression. The basal localization of loss-of-phosphorylation PIN1:GFP increased auxin accumulation in the root tips, partially rescuing *PID* overexpression-induced root collapse. Collectively, our data indicate that reversible phosphorylation of the conserved Ser residues in the PIN1HL by PID (and possibly by other AGC kinases) is required and sufficient for proper PIN1 localization and is thus essential for generating the differential auxin distribution that directs plant development.

INTRODUCTION

The plant hormone auxin plays a central role in almost all aspects of plant development. Unidirectional cell-to-cell transport of auxin generates maxima and minima that are instrumental for tropic growth responses, tissue patterning, and organ initiation (Sabatini et al., 1999; Friml et al., 2002b, 2003; Benkova et al., 2003; Sorefan et al., 2009). The polar auxin flow is accomplished by the concerted action of three families of membrane proteins, the AUXIN RESISTANT1/LIKE AUX1 (AUX1/LAX) influx carriers (reviewed in Parry et al., 2001), the PIN-FORMED (PIN) efflux carriers (reviewed in Paponov et al., 2005), and the P-GLYCO-PROTEIN (PGP/ABCB) transporters (reviewed in Geisler and Murphy, 2006). Until now, the role of the PIN auxin efflux carriers in polar auxin transport is most well established. The *Arabidopsis thaliana* genome encodes eight PIN proteins, named after the *pin-formed/pin1* mutant that is defective in polar auxin transport

and develops pin-shaped inflorescences (Gálweiler et al., 1998). The PIN family proteins can be classified into two groups: (1) the PIN1-type proteins (PIN1, 2, 3, 4, and 7) that are plasma membrane (PM) localized and (2) the PIN5-type proteins (PIN5, 6, and 8) that localize to the endoplasmatic reticulum (ER) and seem to be involved in the regulation of auxin homeostasis (Mravec et al., 2009). The PIN1-type proteins have redundant functions, and a loss-of-function mutation in one *PIN* gene is sometimes compensated for by the ectopic expression of other PINs (Blilou et al., 2005; Vieten et al., 2005). As a result, only mutants in multiple *PIN* genes show more pronounced phenotypes in embryogenesis, root patterning, and lateral root initiation (Benkova et al., 2003; Friml et al., 2003; Blilou et al., 2005).

The PIN1-type proteins determine the direction of cell-to-cell auxin transport through their asymmetric subcellular localization at the PM (Wiśniewska et al., 2006), which is dependent not only on tissue-specific factors, but also on the PIN protein sequence (Wiśniewska et al., 2006). During specific developmental processes, dynamic changes in PIN polarity have been observed (Benkova et al., 2003; Friml et al., 2003; Heisler et al., 2005), and PIN polarity has also been shown to be modulated by environmental cues (Friml et al., 2002b; Harrison and Masson, 2008) and auxin itself (Paciorek et al., 2005; Sauer et al., 2006). Many research efforts have focused on what determines PIN polarity and, thus, what translates upstream developmental and environmental signals into changes in plant architecture by regulating PIN polarity. The current model is that newly synthesized PINs arrive at the PM in a nonpolar fashion and that PIN polarity is established and regulated by subsequent endocytosis,

¹ Current address: Escola Profissional UNIPACS, Rua Guilherme Lahm, 960, Taquara, RS, Brazil.

² Current address: Swammerdam Institute for Life Sciences, University of Amsterdam, Science Park 904, 1098 XH Amsterdam, The Netherlands.

³ Address correspondence to r.offringa@biology.leidenuniv.nl.

The author responsible for distribution of materials integral to the findings presented in this article in accordance with the policy described in the Instructions for Authors (www.plantcell.org) is: Remko Offringa (r.offringa@biology.leidenuniv.nl).

^WOnline version contains Web-only data.

^{OA}Open Access articles can be viewed online without a subscription. www.plantcell.org/cgi/doi/10.1105/tpc.109.072678

transcytosis, and recycling back to the PM (Geldner et al., 2001; Dhonukshe et al., 2008; Kleine-Vehn et al., 2008).

GNOM is a GDP/GTP exchange factor on ADP-ribosylation factor G protein that has been shown to be involved in the recycling of PIN proteins to the basal (root apex facing) side of the PM (Geldner et al., 2003). GNOM is a molecular target of the fungal toxin brefeldin A (BFA), which inhibits protein trafficking and thus interferes with basal PIN1 recycling, leading to PIN1 accumulation into so-called BFA compartments (Geldner et al., 2001). Loss of function of *GNOM* results in severe embryo defects due to disturbance of PIN1 polarity establishment during embryogenesis (Mayer et al., 1993; Steinmann et al., 1999).

Another important molecular determinant in PIN polar targeting is the PINOID (PID) protein Ser/Thr kinase. PID was initially identified through the *Arabidopsis pid* loss-of-function mutants that phenocopy *pin1* mutants (Bennett et al., 1995; Christensen et al., 2000). Both *PID* loss- and gain-of-function mutant phenotypes already indicated a role of PID as a regulator of auxin transport (Benjamins et al., 2001). More recently, PID was shown to act as a binary switch in the apical-basal polar targeting of PIN proteins (Friml et al., 2004). In root cells, *PID* overexpression induces a PIN polarity shift from the basal to the apical (shoot apex facing) side of the cells, leading to agravitropic root growth and collapse of the primary root meristem, due to depletion of the organizing auxin maximum. By contrast, in the inflorescence meristem, *pid* loss of function induces an apical-to-basal shift in PIN1 polarity, which drains the auxin maxima that are necessary for organ initiation, thus resulting in pin-like inflorescences (Friml et al., 2004).

In animal systems, modification of cargo proteins by phosphorylation is an important mechanism to regulate their polar delivery to the PM. For example, in mammalian epithelial cells, phosphorylation of the immunoglobulin receptor at a single Ser residue has been shown to result in its accumulation at the apical cell membrane (Casanova et al., 1990). Protein phosphorylation and dephosphorylation have also been implicated in the regulation of polar auxin transport in plant systems. In tobacco (*Nicotiana tabacum*) suspension cells, the protein kinase inhibitors staurosporine and K252a were found to inhibit auxin efflux (Delbarre et al., 1998), and genetic and pharmacological inhibition of phosphatase activity in *Arabidopsis* led to defects in auxin transport (Garbers et al., 1996; Rashotte et al., 2001). More recent findings revealed that PIN polar localization is determined by reversible phosphorylation of the large central PIN hydrophilic loop (PINHL) through the antagonistic action of the PID kinase and PP2A phosphatases (Michniewicz et al., 2007). This indicated that the machinery of phosphorylation-regulated PM protein polar localization is also operational in plants.

To further elucidate molecular mechanisms of PIN polar localization regulated by PID phosphorylation, we set out to identify the PID phosphorylation targets in the PINHL. Here, we show that the central Ser residues in three conserved TPRXS(N/S) motifs within the PIN1HL are phosphorylated by PID. Inactivation of these phosphosites (nonphosphorylatable or phosphomimic forms) in a complementing *PIN1:GFP* (for green fluorescent protein) construct induced auxin-regulated defects in embryo and inflorescence development that correlated with changes in PIN1:GFP polar localization. Moreover, the localization of loss-

of-phosphorylation and phosphomimic PIN1:GFP proteins in root tips was insensitive to PID overexpression using *P35S:PID*, leading to opposite effects on *P35S:PID*-induced root collapse. Our data indicate that the regulation of PIN1 polar localization through reversible phosphorylation of three conserved Ser residues in the PIN1HL by PID and possibly other AGC kinases is an essential mechanism for aspects of plant development that are directed by differential auxin distribution.

RESULTS

Ser Residues in Three Conserved Motifs in the PIN1HL Are Phosphorylated by PID

The previous observations that the PIN1HL is efficiently phosphorylated by PID in vitro (Michniewicz et al., 2007) prompted us to map PID phosphorylation targets in the PIN1HL. Analysis of the PIN1 amino acid sequence using the NetPhos program (Blom et al., 1999) identified 23 putative phosphosites, 20 of which are located in the PIN1HL (see Supplemental Figure 1 online). Twelve synthetic peptides comprising 17 putative phosphosites were tested in in vitro phosphorylation assays, and six were found to be highly phosphorylated by PID (see Supplemental Figure 2 online).

Since the PID-dependent basal-to-apical switch in PIN polarity is not restricted to PIN1, but is also observed for PIN2 and PIN4 (Friml et al., 2004), we aligned the amino acid sequences of six PIN proteins (PIN1, 2, 3, 4, 6, and 7) in which a clear hydrophilic loop (HL) can be identified. Eleven of the NetPhos predicted Ser (S) and Thr (T) residues showed conservation among the six *Arabidopsis* PIN proteins (indicated with an asterisk in Figure 1), five of which appeared to be fully conserved (labeled in black and with an asterisk in Figure 1). Interestingly, these five residues were located in the highly phosphorylated peptides 2, 6, 8, and 12 (see Supplemental Figure 2 online), and two of them (Thr-227 and Ser-290) were recently reported to be modified by phosphorylation in vivo (Benschop et al., 2007). We noted that S290 was located in a TPRXS motif that was conserved among the six PIN proteins (Figure 1) and resembled the consensus phosphorylation site of the animal AGC kinase, protein kinase A (PKA). Therefore, we first tested whether Ser-290 is a PID phosphorylation target by replacing this Ser with Ala in a HIS-tagged short version of the PIN1HL (PIN1HLsv) (see Supplemental Figure 1 online) and incubating wild type or mutant proteins with HIS-tagged PID in an in vitro phosphorylation reaction. Clear PID autophosphorylation and PID-dependent phosphorylation of HIS-PIN1HLsv was detected (see Supplemental Figure 3A online). The S290A substitution reduced PIN1 phosphorylation by PID to a background level (see Supplemental Figure 3A online), indicating that Ser-290 is a PID phosphorylation target. Two additional TPRXS(N/S) motifs were identified upstream of Ser-290 (Figure 1), and the Ser residue (Ser-252) of the second motif was also shown to be modified by phosphorylation in vivo (Benschop et al., 2007). For convenience in our experiments, we refer to the Ser residues at positions 231, 252, and 290 as S1, S2, and S3, respectively (Figure 1).

We next tested the effect of Ser-to-Ala substitution (S1A, S2A, S3A, or combinations) on PID phosphorylation using a

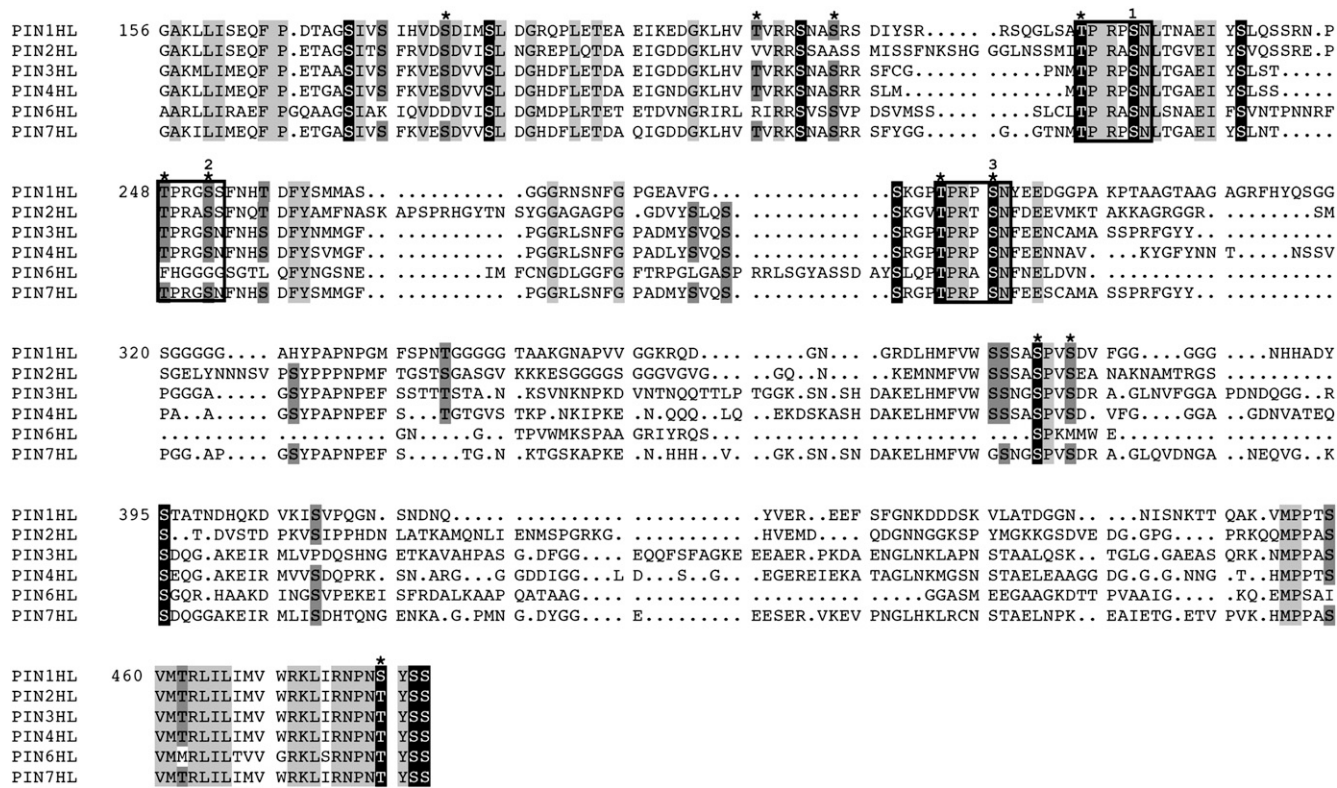


Figure 1. Alignment of the Amino Acid Sequences of the HL of Six *Arabidopsis* PIN Proteins.

Conserved Ser or Thr residues predicted by NetPhos to be phosphorylated are indicated by asterisks. Residues that are conserved in all six PINHLs are blocked with black (Ser and Thr residues) or light gray (other amino acids). Residues that are conserved in four or five of the six PINHLs are blocked with dark gray. The three TPRXS(N/S) motifs are boxed, and the Ser residues at positions 231, 252, and 290 within these motifs are renumbered to 1, 2, and 3, respectively.

glutathione S-transferase (GST)-tagged version of the full-length PIN1HL. Under our experimental conditions, the GST-PIN1HL was unstable, showing a reproducible pattern of degradation bands. A single S1A or S3A substitution led to a 40 or 20% reduction, respectively, double S1,2A and S1,3A substitutions led to a 50% reduction, and triple S1,2,3A substitutions led to an 80% reduction of phosphorylation by PID compared with the wild-type PIN1HL (Figure 2B). These data indicated that the central Ser residues within the three highly conserved TPRXS(N/S) motifs are targets for PID phosphorylation in vitro.

At the same time, the PIN1HL S1,3A double substitution construct was used to test all other Ser and Thr residues located in the highly phosphorylated peptides 2 (T227), 6 (T286), 8 (S377 and S380), 11 (T458 and S459), and 12 (S479) (see Supplemental Figure 2 online). Based on the relative intensities of the phosphorylated bands, substitution of these amino acids with Ala residues had no clear effect on PID phosphorylation (see Supplemental Figures 3B and 3C online), indicating that these residues are not phosphorylated by PID.

BLAST analysis of the *Arabidopsis* protein database (<http://www.ncbi.nlm.nih.gov/protein/>) showed that TPRXS(N/S) is a PIN-specific motif. Strikingly, alignment of amino acid se-

quences of PIN1 proteins from five different plant species (Xu et al., 2005; Carraro et al., 2006) showed that the three identified motifs are highly conserved, even in the moss *Physcomitrella patens* (see Supplemental Figure 4 online), suggesting their functional conservation throughout the evolution of land plants.

Loss of PIN1 Phosphorylation at the Conserved Ser Residues Induces Dominant Embryo and Flower Phenotypes

To investigate the biological significance of the PIN1 phosphorylation in planta, various mutant constructs were generated from *PPIN1* (*PIN* promoter):*PIN1:GFP* (hereafter referred to as *PIN1:GFP*), in which one, two, or all three Ser residues in the encoded PIN1:GFP proteins were replaced by Ala (A), a nonphosphorylatable residue, or by Glu (E) to mimic phosphorylation. The resulting constructs *PIN1:GFP S1A(E)*, *PIN1:GFP S3A(E)*, *PIN1:GFP S1,3A(E)*, and *PIN1:GFP S1,2,3A(E)* were transformed into *Arabidopsis* Columbia (Col) wild-type plants, and GFP positive, single locus insertion lines were selected for analysis. A previously described *PIN1:GFP* line (Benkova et al., 2003) was used as the control.

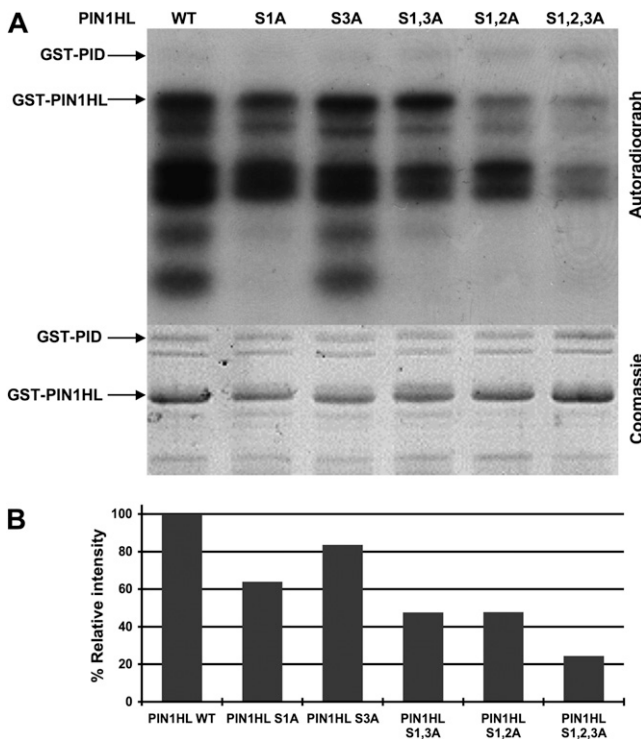


Figure 2. Ser Residues in Three Conserved Motifs within the PIN1HL Are Phosphorylated by PID in Vitro.

(A) In vitro assay of phosphorylation by GST-PID kinase using wild-type GST-PIN1HL and mutant protein substrates in which the indicated Ser residues (S1, S2, or S3) were replaced with Ala residues **(A)**. The positions of GST-PID and the full-length GST-PIN1HL are indicated in the autoradiograph (top panel) and the Coomassie-stained gel (bottom panel). Autophosphorylation of GST-PID can be observed in the top panel. Under our experimental conditions, *Escherichia coli*-purified GST-PIN1HL was not stable, resulting in a reproducible pattern of degradation bands. The Coomassie blue-stained gel was used as a control for protein loading.

(B) Quantitative assessment of the in vitro phosphorylation assay in **(A)**. The phosphorylation intensity is expressed as the percentage of phosphorylation relative to the wild-type GST-PIN1HL protein. Numbers were corrected for protein loading based on analysis of the Coomassie blue-stained blot.

The *PIN1:GFP S→E* and *PIN1:GFP S3A* plants showed largely normal development at seedling and flowering stage. By contrast, other mutants exhibited a range of dominant defects. The *PIN1:GFP S1A* and *PIN1:GFP S1,3A* mutants showed cotyledon number defects, reflected by seedlings having one, three, or four cotyledons (Figures 3D to 3F), with the three-cotyledon phenotype characteristic of the *pid* loss-of-function mutant (Figure 3B) predominating. For these two mutant constructs, two lines each were selected for detailed analyses, one with a lower *PIN1:GFP* expression level (*PIN1:GFP S1A#14* and *PIN1:GFP S1,3A#12*) and one with a higher *PIN1:GFP* expression level (*PIN1:GFP S1A#15* and *PIN1:GFP S1,3A#10*) (see Supplemental Figure 5A online). Notably, the stronger lines showed higher frequencies of cotyledon defects (e.g., *PIN1:GFP S1A#15*: 21.7%, $n = 757$) than

the weaker lines (e.g., *PIN1:GFP S1A#14*: 12.5%, $n = 654$) (Figure 3N), indicating that the severity of the cotyledon phenotypes corresponded to the level of mutant *PIN1:GFP* protein expression. The stronger lines *PIN1:GFP S1A#15* and *PIN1:GFP S1,3A#10* developed flowers with an increased number of petals and a decreased number of stamens and carpels (Figure 4B, Table 1), mimicking *pid* mutant floral defects (Figure 4A, Table 1) (Bennett et al., 1995).

To exclude other possible reasons for the observed dominant phenotypes, such as cosuppression, the protein levels of the transgene and the endogenous *PIN1* gene were quantified by protein gel blot analysis. All transgenic lines showed endogenous *PIN1* expression similar to that of the wild type, and the mutant *PIN1:GFP* expression levels of the strong lines were comparable to that of the *PIN1:GFP* control line (see Supplemental Figure 5B online). These results showed similar protein expression of both endogenous *PIN1* and *PIN1:GFP*, suggesting that the dominant developmental defects observed can be attributed to the expression of the mutant *PIN1:GFP* proteins that outcompete endogenous *PIN1*, possibly by differential localization at the PM.

For the *PIN1:GFP S1,2,3A* triple substitution lines, the post-embryo defects were more severe. No homozygous progeny could be obtained, and approximately one-fourth of the seeds from heterozygous plants (25.6%, $n = 156$ for line #23) failed to germinate, indicating that the homozygous progeny are embryo lethal. Among the germinating seedlings, we occasionally (9.6%, $n = 156$ for line #23) observed strong patterning defects (indicated as “others” in Figures 3N and 3O), such as seedlings without a root (Figures 3G and 3H) or ball-shaped structures without any discernible apical-basal axis that stopped growing after germination (Figures 3I and 3J).

Reversible Phosphorylation of the Conserved Ser Residues Is Necessary and Sufficient for Proper PIN1 Localization and Plant Development

To further test the functionality of the loss- or gain-of-phosphorylation *PIN1:GFP* proteins, the *PIN1:GFP* and *PIN1:GFP S→A(E)* mutant lines were crossed with the *pin1* loss-of-function mutant, and where possible, double homozygous plants were selected for analysis. The *pin1* mutant has aberrant cotyledon numbers (Figures 3C, 3N, and 3O) and pin-formed inflorescences with no flowers or only a few defective flowers (Okada et al., 1991). In our analyses, *PIN1:GFP*, as well as *PIN1:GFP S1E*, *PIN1:GFP S3E*, and *PIN1:GFP S1,3E*, complemented *pin1* cotyledon and inflorescence defects (Figures 3O, 4C, and 4D). *PIN1:GFP S1A* and *PIN1:GFP S3A* partially rescued *pin1* defects, reflected by a reduced frequency of *pin1* cotyledon defects from 17.6% ($n = 318$) to 2% ($n = 402$) and 12.1% ($n = 348$), respectively (Figure 3O), and by the observations that no pin-formed inflorescences were produced (Figures 4F and 4G). By contrast, *PIN1:GFP S1,3A* and *PIN1:GFP S1,2,3A(E)* lines showed an enhanced frequency (23.9% $n = 351$, 32.7% $n = 110$, and 71.2% $n = 66$, respectively; Figure 3O) and severity of seedling defects, such as cup-shaped cotyledons (3.5%; Figure 3K) or no cotyledons (2%; Figure 3L), phenotypes typical for the *pin1 pid* double mutant (Furutani et al., 2004) but not for

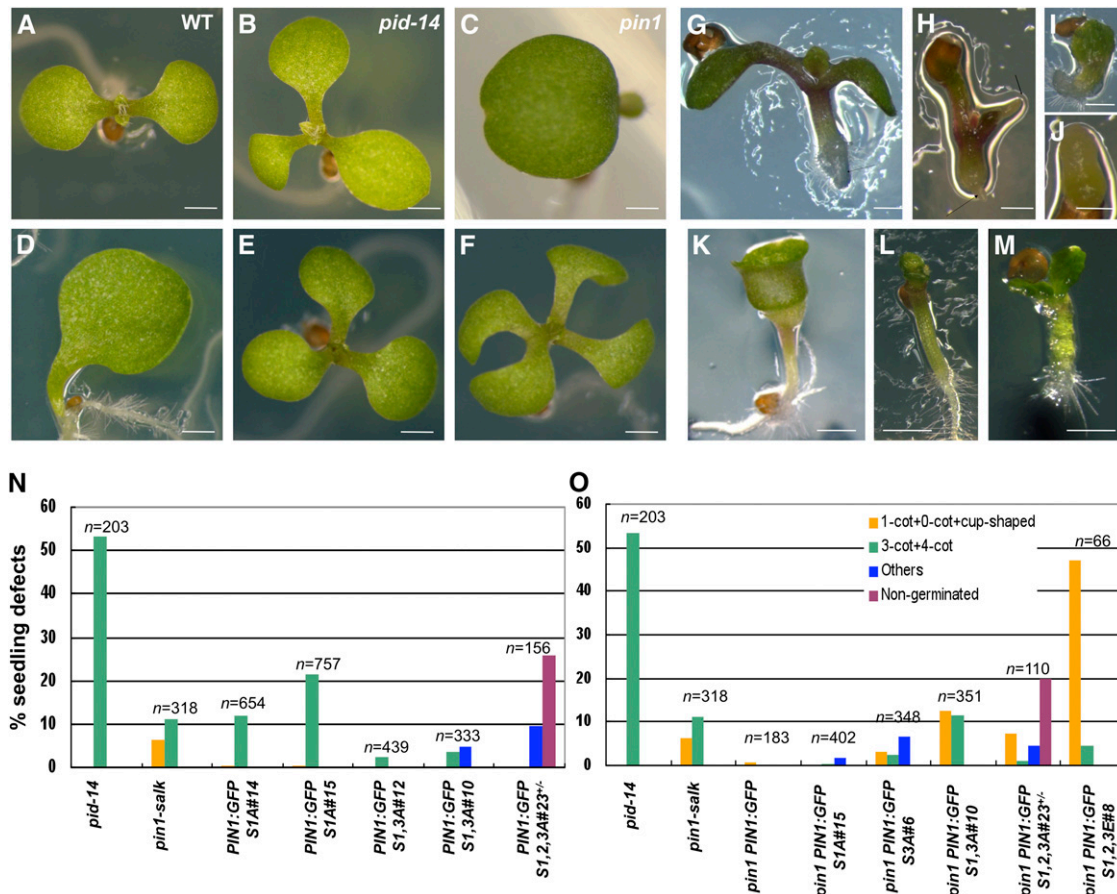


Figure 3. Seedling Phenotypes Induced by Manipulation of the Conserved Ser Residues in PIN1:GFP.

(A) to (F) Cotyledon number defects observed in *pid-14* (B), *pin1* (C), and *PIN1:GFP S1A* (D) to (F) mutant seedlings compared with a wild-type seedling (A).

(G) to (J) Progeny from *PIN1:GFP S1,2,3A#23^{+/−}* plants showing severe patterning defects, such as seedling without a root (G) and (H), with reduced cotyledons (H), or oblong structures (I) and (J).

(K) to (L) Cotyledon defects observed in *pin1 PIN1:GFP S1,3A#10* mutant seedlings showing a cup-shaped cotyledon (K) or no cotyledons (L).

(M) Progeny from *pin1^{+/−} PIN1:GFP S1,2,3A#23^{+/−}* plants showing callus-like hypocotyl and cotyledons lacking a primary root. Bars in (A) to (M) = 10 μ m.

(N) and (O) Quantitative analysis of seedling defects induced by expression of the phosphomutant *PIN1:GFP* versions in the wild-type background (N) and in *pin1* mutant background (O). The number of seedlings scored per mutant line is indicated. The legends in (O) are also used for (N). “Others” represents phenotypes other than cotyledon number defects, such as seedling without root, oblong structures, or callus-like seedlings.

the *pid* or *pin1* single mutant (Figures 3N and 3O). Around 5% of the progeny from *pin1^{+/−} PIN1:GFP S1,2,3A^{+/−}* (double heterozygous) plants lacked a primary root and developed callus-like hypocotyls and cotyledons (Figure 3M). At the flowering stage, *PIN1:GFP S1,3A* and *PIN1:GFP S1,2,3A* (E) mutants could not complement *pin1* defects and produced pin-like inflorescences, with *pin1 PIN1:GFP S1,2,3E* occasionally forming flowers producing seeds (Figure 4E). The *pin1 PIN1:GFP S1,3A* inflorescences were branched and formed sterile flowers with fused petals (Figure 4H), whereas *pin1 PIN1:GFP S1,2,3A^{+/−}* plants only produced a single needle-shaped inflorescence (Figure 4I).

Next, we examined whether these mutant defects correlated with changes in the subcellular localization of the mutant *PIN1:GFP* proteins. Consistent with previous observations (Friml et al.,

2004), in auxin transport inhibitor-induced pin-shaped inflorescence apices, *PIN1:GFP* was localized apically in the epidermis (Figure 5A). In a comparable region of the pin-shaped inflorescence apex, the phosphomimetic *PIN1:GFP S1,2,3E* protein also showed apical localization (Figure 5B), whereas the *PIN1:GFP S1,3A* and *PIN1:GFP S1,2,3A* proteins were targeted to the basal side (Figures 5C and 5D), similar to *PIN1* localization in *pid* mutant (Friml et al., 2004).

Collectively, these data indicated that *PIN1* loss of phosphorylation results in its basal localization, whereas phosphomimicking induces apical targeting of *PIN1* in the shoot apical meristem, both leading to failure to complement the *pin1* mutant phenotypes. These observations are consistent with the identified role for *PID* as a binary switch in *PIN1* basal-apical polar



Figure 4. Inflorescence and Flower Defects Observed after Expression of Phosphomutant PIN1:GFP Proteins.

(A) and (B) Flowers of the *pid-14* loss-of-function mutant (A) and the *PIN1:GFP S1,3A#10* mutant (B) show similar defects. (C) to (I) Complementation analysis of *pin1* loss-of-function mutant inflorescence and flower defects. *PIN1:GFP* (C) and *PIN1:GFP S1,3E#18* (D) fully rescued pin-shaped inflorescence defects, whereas *PIN1:GFP S1A#15* (F) and *PIN1:GFP S3A#6* (G) only partially rescued pin-shaped inflorescence defects. *PIN1:GFP S1,2,3E#8* (E), *PIN1:GFP S1,3A#10* (H), and *PIN1:GFP S1,2,3A#23* (I) did not rescue *pin1* inflorescence defects. Insets show details of flower morphology and pin-like inflorescences. Bars in whole-plant photographs = 5 cm.

localization in the shoot apex, suggesting that the identified Ser residues are PID related.

Strong Embryo Defects Are Induced by PIN1:GFP S1,2,3A Mislocalization

The embryo and seedling lethality observed in the progeny of *pin1^{+/−} PIN1:GFP S1,2,3A^{+/−}* plants led us to study the early embryo development. Compared with *pin1 PIN1:GFP* embryos that showed stereotypic patterns of cell divisions (Figure 6A), ~30% ($n = 86$) of the embryos from *pin1^{+/−} PIN1:GFP S1,2,3A^{+/−}* plants exhibited a range of developmental aberrations at different stages (Figure 6B). In 15% of the embryos, the basal tier and suspensor cells showed defective cell divisions. The most severe cases were characterized by embryos with globular structures that lacked a defined apical-basal axis and bilateral symmetry

(5%). These embryo phenotypes resembled those of mutants with defects in auxin transport (Friml et al., 2003) and *gnom* mutants (Mayer et al., 1993).

Examination of the subcellular localization of *PIN1:GFP S1,2,3A* during embryogenesis showed that *PIN1:GFP S1,2,3A* polarity failed to establish properly ($n = 43$). Endogenous *PIN1* (or wild-type *PIN1:GFP*) proteins localize at the basal side of the provascular cells (Figure 6C), generating an auxin maximum that defines the hypophyseal cell group (Figure 6F) and at the apical side of the epidermal cells from triangular stage on (Figure 6C and inset), generating strong auxin activity at tips of developing cotyledons (Steinmann et al., 1999; Friml et al., 2003). In embryos from *pin1^{+/−} PIN1:GFP S1,2,3A^{+/−}* plants with a largely wild-type morphology (65%, $n = 43$), the basal *PIN1:GFP* localization in the provascular cells was lost (Figure 6D, star), causing a reduction of the auxin reporter *PDR5:GFP* signal in the hypophysis (Figure

Table 1. Quantitative Analysis of Dominant *pid*-Like Floral Organ Defects Induced by *PIN1:GFP S→A*

Genotype	Floral Organ Numbers				Total No. of Flowers
	Sepal	Petal	Stamen	Carpel	
Col	4.00	4.00	5.80 ± 0.40	2.00	50
<i>pid-14</i>	2.80 ± 1.20	8.35 ± 1.42	1.10 ± 1.07	0.00	20
<i>PIN1:GFP S1A#15</i>	4.11 ± 0.68	5.53 ± 0.63	4.91 ± 0.85	1.52 ± 0.57	45
<i>PIN1:GFP S1,3A#10</i>	4.08 ± 0.68	5.71 ± 1.09	4.15 ± 0.87	1.83 ± 0.33	52

Numbers are means derived from analyses of flowers from at least five plants for each genotype. Standard deviations are indicated. In the case of organ fusion in the same whorl, a fused floral organ is counted as one in that whorl. In the case of organ fusion between different whorls, fused organs are counted as one organ in the each whorl.

6G). As a comparison, the basal localization of *PIN1:GFP S1,3A* in the provascular cells was not changed (see Supplemental Figure 6A online). In embryos exhibiting strong defects, *PIN1:GFP S1,2,3A* polarity was dramatically disrupted, and abundant intracellular signal was observed (Figure 6E). The cells with the fluorescent signal at the PM showed no polarity or randomized polarity (see Supplemental Figures 6B and 6C online), and a clear *PDR5:GFP* maximum was not detected (Figure 6H).

These data implied that phosphorylation of the three Ser residues is required for auxin-related embryo development by regulating *PIN1* PM localization.

PIN1 Phosphorylation at the Conserved Ser Residues Is Related to PID Activity

Above, we showed that the conserved Ser residues are phosphorylated by PID in vitro and that PID regulation of *PIN1* polarity and the resulting inflorescence development (Friml et al., 2004)

can be mimicked by manipulation of these Ser residues. For additional confirmation that our identified phosphoserines are targets of PID activity in vivo, we crossed the *PIN1:GFP*, *PIN1:GFP S1,3A*, and *PIN1:GFP S1,2,3E* lines with the strong *PID* overexpression line *P35S:PID#21* (Benjamins et al., 2001). The *PIN1:GFP S1,2,3A* line could not be used for this purpose, as it could only be maintained in the heterozygous state, which precluded an equivalent comparison of the root meristem collapse frequency.

In line with our previous observations (Friml et al., 2004), *PID* overexpression induced a clear basal-to-apical shift of *PIN1:GFP* localization in root stele cells (Figures 7A and 7B). By contrast, *PIN1:GFP S1,3A* showed basal localization in both wild-type and *P35S:PID* backgrounds (Figures 7C and 7D). Simultaneous immunolocalization showed the basal-to-apical polarity shift of *PIN2* in the cortex and *PIN4* in the root meristem (Figure 7M), demonstrating that *PID* overexpression was sufficient to induce *PIN* polarity shifts and that the *S1,3A* substitutions rendered

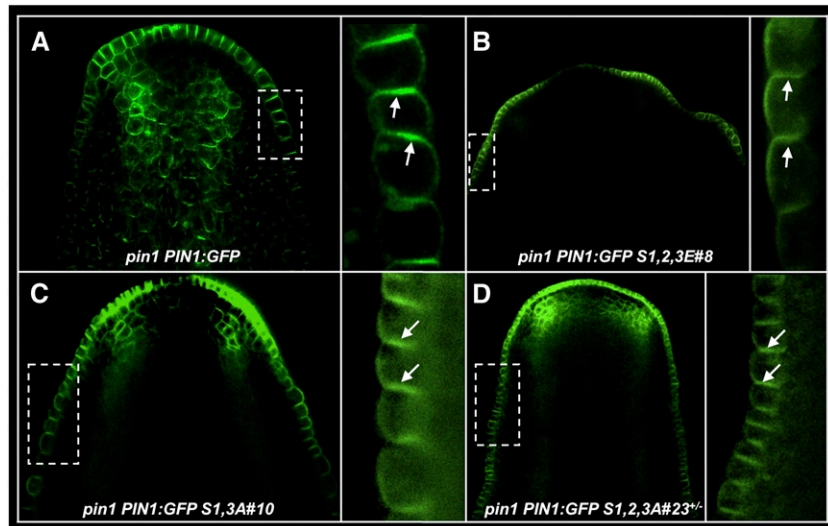


Figure 5. Subcellular Localization of Wild-Type and Phosphomutant *PIN1:GFP* Proteins in Epidermal Cells of the Inflorescence Apex.

Confocal laser scanning microscopy of pin-formed inflorescence apices of *pin1* mutant plants expressing wild-type *PIN1:GFP* (naphthylphthalamic acid treated) (A), *PIN1:GFP S1,2,3E* (B), *PIN1:GFP S1,3A* (C), and *PIN1:GFP S1,2,3A* (D). The white dashed boxes in the overview images (left) indicate the position of the zoomed-in images (right). The polarity of *PIN1:GFP* in the epidermal cells of the inflorescence apex is indicated with arrows. *PIN1:GFP S1,2,3A#23^{+/-}* indicates that the plant is heterozygous for the transgene.

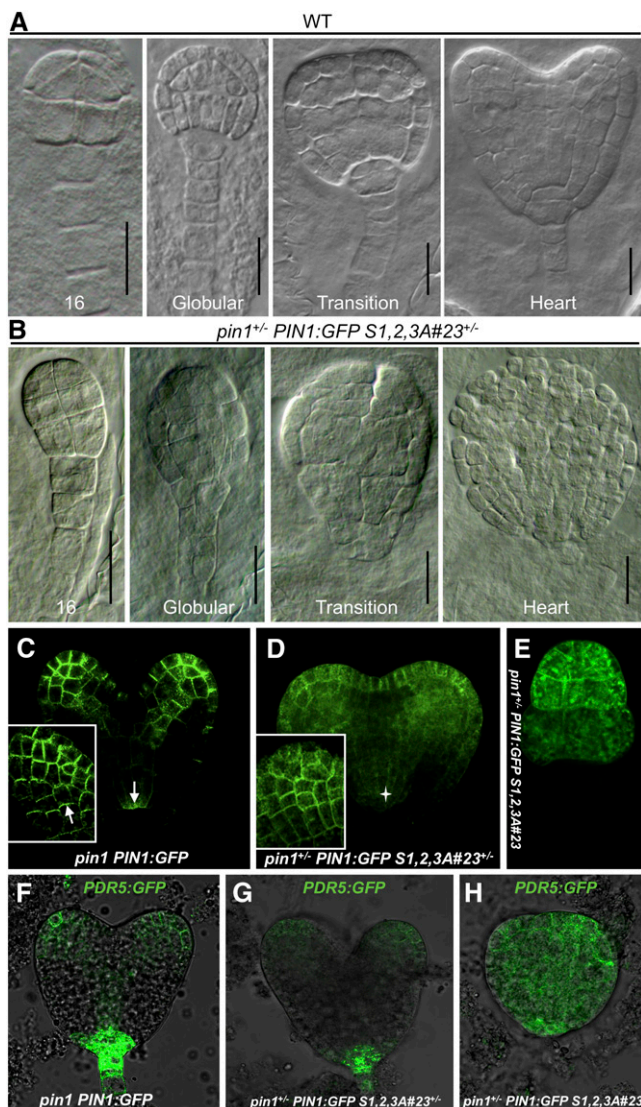


Figure 6. Embryo Defects Induced by PIN1:GFP S1,2,3A Mislocalization Are Due to Disturbed Auxin Distribution.

(A) and **(B)** Differential interference contrast microscopy images of embryos from wild-type **(A)** and *pin1^{+/−} PIN1:GFP S1,2,3A#23^{+/−}* **(B)** plants. Text at the bottom of each image indicates the developmental stage of the embryo. For the defective embryos in **(B)**, the developmental stage was based on a rough estimate of the cell number. Bars = 10 μ m. **(C)** to **(E)** Confocal laser scanning microscopy images of *pin1 PIN1:GFP* heart-stage embryos **(C)** and wild-type looking **(D)** and defective looking **(E)** embryos from *pin1^{+/−} PIN1:GFP S1,2,3A#23^{+/−}* plants from the same developmental stage. Insets in **(C)** and **(D)** represent confocal scans through the epidermal cell layer of cotyledon primordia. White arrows in **(C)** and **(D)** indicate the PIN1:GFP polarity, and a star in **(D)** indicates the absence of basally localized PIN1:GFP S1,2,3A protein. **(F)** to **(H)** Confocal laser scanning microscopy images of *PDR5:GFP* auxin distribution in embryos from *pin1 PIN1:GFP* **(F)** and *pin1^{+/−} PIN1:GFP S1,2,3A#23^{+/−}* **(G)** and **(H)** plants, showing a reduced **(G)** or mislocalized **(H)** auxin maximum.

PIN1:GFP insensitive to that. On the other hand, the PIN1:GFP S1,2,3E protein exhibited apical localization in some cell files and apolar localization in others in both wild-type and *P35S:PID* backgrounds (Figures 7E and 7F), further indicating that the polar localization of the phosphorylation mutant PIN1:GFP proteins occurred independent of *PID* overexpression. Consistent with the PIN1 function of mediating auxin transport to root tips, *PIN1:GFP S1,3A* induced an enhancement of auxin reporter *PDR5:GFP* signal compared with the control *PIN1:GFP* roots (Figures 7G and 7I; see Supplemental Figure 7 online; Student's *t* test, $P < 0.05$), consistent with the basal localization of PIN1:GFP S1,3A protein. By contrast, the *PDR5:GFP* signal was significantly reduced in *PIN1:GFP S1,2,3E* root tips (Figure 7K; see Supplemental Figure 7 online; Student's *t* test, $P < 0.05$), in line with its preferably apical localization.

In the *P35S:PID* background, basally accumulated PIN1:GFP S1,3A resulted in higher auxin accumulation compared with *PIN1:GFP* (Figures 7J and 7H; see Supplemental Figure 7 online; Student's *t* test, $P < 0.05$) and as a result significantly reduced the *P35S:PID*-induced root collapse frequency (Figure 7N). By contrast, *PIN1:GFP S1,2,3E* had no significant effect on *P35S:PID*-induced root collapse (Figure 7N). This might be due to the already maximal effect of *PID* overexpression on PIN apicalization and auxin depletion, as no significant reduction of auxin accumulation was detected (Figures 7B and 7F; see Supplemental Figure 7 online). The genetic interactions between phosphomutants and *PID* confirmed that our identified Ser residues are phosphotargets of *PID*.

Together, these results linked phosphorylation of the conserved Ser residues to polar PIN1 driven differential auxin distribution in roots and further demonstrated that the conserved phosphoserines are key determinants in modulating plant architecture by instructing PIN1 polarity.

DISCUSSION

Previously, it has been shown that the *PID* kinase and PP2A phosphatases antagonistically regulate PIN polarity by reversible phosphorylation of the PIN1HL (Michniewicz et al., 2007). However, no functional evidence was provided to support the importance of this phosphorylation in planta. In this study, we identified Ser residues centrally located in three conserved TPRXS(N/S) motifs within the PIN1HL that are phosphorylated by *PID* in vitro. Subsequent *in planta* analyses of loss-of-phosphorylation and phosphomimic *PIN1:GFP* mutants proved that reversible phosphorylation of all three residues is required and sufficient for proper PIN1 polar localization and auxin-regulated plant development.

Ser Residues in the Conserved TPRXS(N/S) Motifs Are Crucial Phosphorylation Targets in the PIN1HL

Several Ser and Thr residues within the PIN1HL have been identified as phosphorylation substrates *in vivo*, and not surprisingly, S2 and S3 are among them (Nühse et al., 2004; Benschop et al., 2007). Two other phosphorylation targets in the PIN1HL identified by mass spectrometry analysis are Ser-337 and

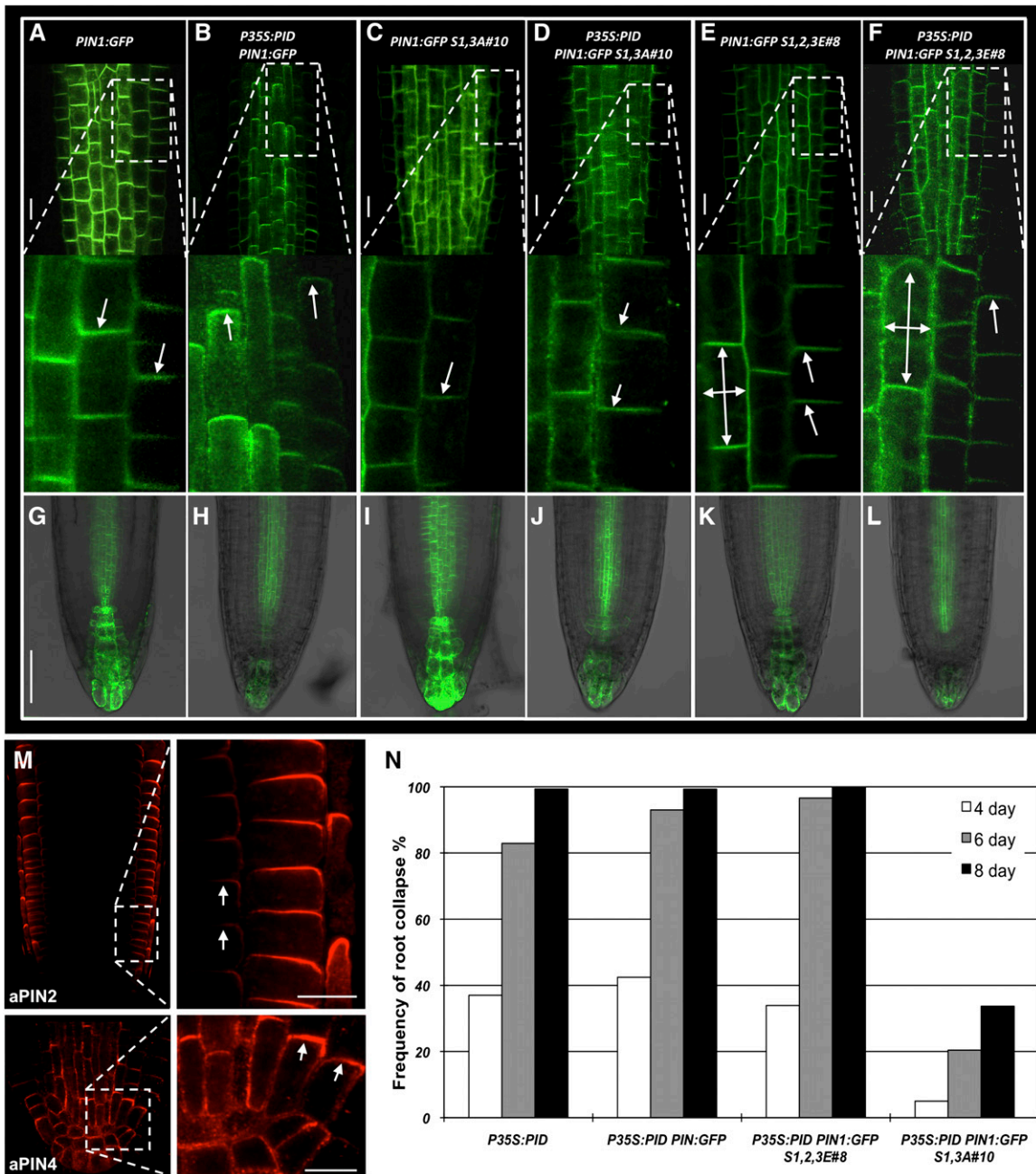


Figure 7. PIN1:GFP Polarity Changes Induced by Manipulation of Phosphoserines Correlate with Changes in the Auxin Maximum in the Root Tip.

(A) to (F) Confocal laser scanning microscopy of primary roots of 5-d-old seedlings expressing PIN1:GFP ([A] and [B]), PIN1:GFP S1,3A#10 ([C] and [D]), and PIN1:GFP S1,2,3E#8 ([E] and [F]) in the wild-type ([A], [C], and [E]) or P35S:PID ([B], [D], and [F]) background. The white dashed boxes in the overview images (top) indicate the position of the zoomed-in images (bottom), in which the PIN1:GFP polarity is indicated by arrows. The seedlings are homozygous for the indicated T-DNA constructs. Bars = 5 μ m.

(G) to (L) Confocal laser scanning microscopy of PDR5:GFP signals in 3-d-old seedling root tips expressing PIN1:GFP ([G] and [H]), PIN1:GFP S1,3A#10 ([I] and [J]), and PIN1:GFP S1,2,3E#8 ([K] and [L]) in the wild-type ([G], [I], and [K]) or P35S:PID ([H], [J], and [L]) background. The seedlings are heterozygous for the PDR5:GFP reporter. Bar = 50 μ m.

(M) PIN2 and PIN4 immunolocalization in 3-d-old P35S:PID PIN1:GFP S1,3A#10 seedling roots. The arrows indicate the apical PIN2 and PIN4 localization induced by PID overexpression. Bars = 5 μ m.

(N) Quantification of the effects of wild-type, loss-of-phosphorylation, or phosphomimic PIN1:GFP expression on the PID overexpression-induced root meristem collapse phenotype. Percentages are based on scoring 153, 144, 179, and 98 seedlings at 4, 6, and 8 d after germination.

Thr-340 in the **MFS**PNTG sequence (Benschop et al., 2007; Michniewicz et al., 2007). Recent functional analysis of these residues in planta has shown that their phosphorylation states are important for PIN1 polarity (Zhang et al., 2010). However, these residues are not directly phosphorylated by PID (Zhang et al., 2010), suggesting that other protein kinases could coordinately regulate PIN polarity with PID by phosphorylating Ser-337 and Thr-340. Ser-337 could be a target of mitogen-activated protein kinases (Benschop et al., 2007), as mitogen-activated protein kinases preferably phosphorylate Ser or Thr residues followed by a Pro in both plant and animal systems (Pearson et al., 2001; Liu and Zhang, 2004).

The TPRXS(N/S) motifs in the HL are highly conserved among six *Arabidopsis* PIN proteins (Figure 1) and among PIN1 homologs from other land plant species (see Supplemental Figure 4 online), suggesting functional conservation of the motifs. Interestingly, PID orthologs have been identified in maize (*Zea mays*) and rice (*Oryza sativa*; McSteen et al., 2007; Morita and Kyozuka, 2007), and it has been shown that the maize ortholog BARREN INFLORESCENCE2 phosphorylates Zm PIN1a, the maize ortholog of *Arabidopsis* PIN1 in vitro, and that it regulates the subcellular localization of Zm PIN1a in vivo (Skirpan et al., 2009). Further research is needed, however, to establish whether this functional conservation extends to the conserved TPRXS(N/S) motifs in all PIN1-type proteins in *Arabidopsis* and in other plant species.

For the *Arabidopsis* PIN1-type proteins (PIN1, 2, 3, 4, and 7), the predicted protein structure consists of two sets of five transmembrane domains that are linked by a HL (Gälweiler et al., 1998; Müller et al., 1998). On the other hand, for the PIN5-type proteins (PIN5, 6, and 8), two sets of five and four transmembrane domains, respectively, are predicted (Mravec et al., 2009). PIN5 and PIN8 clearly lack a large central HL (Mravec et al., 2009), but our alignment suggests that a shorter HL is present in PIN6 and that it contains two TPRXS(N/S) motifs (Figure 1). Immunohistochemical analyses and studies using reporter fusion proteins have shown that PIN1, 2, 3, 4, and 7 are localized at the PM (Gälweiler et al., 1998; Müller et al., 1998; Friml et al., 2002a, 2002b, 2003), whereas PIN5, 6, and 8 are ER localized (Mravec et al., 2009). This suggests that for ER-localized PIN proteins, there has been no selective advantage to maintain PINHL-located polarity determinants. Alternatively, the loss of phosphorylation motifs may have been crucial for allowing the diversification of PIN proteins function from the PM to the ER.

Phosphorylation of the Conserved Ser Residues Directs PIN1 Polar Localization and Auxin-Regulated Plant Development

In wild-type plants, PIN1 proteins are basally localized in (pro)vascular tissues in embryos, leaves, and roots and are apically localized in the epidermis of shoot apices and embryos (Gälweiler et al., 1998; Benkova et al., 2003; Friml et al., 2003, 2004; Reinhardt et al., 2003). Our analyses of the subcellular localization of mutant PIN1:GFP proteins in different tissues showed that manipulation of the phosphoserines leads to changes in PIN1 polarity, most (but not all) of which are consistent with the PID binary switch function (Friml et al., 2004).

In the epidermis of the shoot apex, loss-of-phosphorylation PIN1:GFP S1,3A and PIN1:GFP S1,2,3A proteins were targeted to the basal side (Figures 5C and 5D), whereas the phosphomimic PIN1:GFP S1,2,3E protein was apicalized (Figure 5B). This pattern is consistent with the binary switch mode, which proposes that no or low kinase activity (in the *pid* mutant) results in PIN1 localization at the basal membrane and that above threshold kinase activity (in the wild type) directs PIN1 apical localization (Friml et al., 2004). Despite its apical localization, PIN1:GFP S1,2,3E could not complement *pin1* inflorescence defects (Figure 4E), a result that is seemingly contradictory to the observation that in the shoot apex of wild-type plants, PIN1 is apically localized. However, PIN1 polarity and the resulting auxin maxima in the shoot apex have been reported to be highly dynamic (Heisler et al., 2005), and a constitutively apical-localized PIN1:GFP S1,2,3E would obviously interfere with auxin-mediated organ initiation. In addition, the shoot defects could also be attributable to PIN1:GFP S1,2,3E apical localization in the vascular tissues where PIN1 polarity is normally basal.

In seedling roots, loss-of-phosphorylation PIN1:GFP S1,3A was localized on the basal membrane of root stele cells, in both the wild type and *P35S:PID* background (Figures 7C and 7D), indicating that the protein is unresponsive to PID activity. Even though endogenous PIN2 and PIN4 in the same roots underwent the basal-to-apical polarity shift induced by PID overexpression (Figure 7M), the root collapse was delayed (Figure 7N). Previously, we have shown that *pin2* and *pin4* loss-of-function mutants delay *P35S:PID*-mediated root meristem collapse (Friml et al., 2004). It is therefore not surprising that the basally localized phosphorylation-deficient PIN1 is able to reduce the frequency of root meristem collapse.

By contrast, PIN1:GFP S1,2,3E was preferably targeted to the apical membrane of root stele cells (Figure 7E). It has been shown that apical localized PIN proteins are more resistant to BFA-induced internalization (Kleine-Vehn et al., 2008). Consistently, PIN1:GFP S1,2,3E was more resistant to BFA treatment than wild-type PIN1:GFP (Kleine-Vehn et al., 2009). This, together with the reduction of the *PDR5:GFP* signal in root tips compared with that in *PIN1:GFP* roots (Figures 7K and 7G; see Supplemental Figure 7 online; Student's *t* test, $P < 0.05$), strongly support that PIN1:GFP S1,2,3E predominantly localizes to the apical membrane. The apical localization of phosphomimic PIN1:GFP did not induce root meristem collapse on its own. This can be explained by the fact that the PID overexpression-induced root meristem collapse is caused by the basal-to-apical polarity change of three PIN proteins (PIN1, PIN2, and PIN4), of which PIN2 and PIN4 are crucial players (Friml et al., 2004).

Moreover, PIN1:GFP S1,2,3E apicalization was not complete, as in certain cell files, apolar PIN1:GFP S1,2,3E localization was also detected (Figures 7E and 7F). Possibly, Glu is not a perfect phosphomimic in these cell files. Alternatively, there could still be additional PID phosphorylation targets in the PIN1HL, as the S1,2,3A mutations did not completely abolish PID phosphorylation of the PIN1HL in vitro. Nonetheless, the basal localization of loss-of-phosphorylation PIN1 and the apical localization of phosphomimic PIN1, together with their opposite effects on PID overexpression-induced root collapse, indicated that our identified phosphoserines are functional targets of PID.

During embryogenesis, phosphorylation of the conserved Ser residues seems to play a role in the maintenance of PIN1 PM localization rather than polarity alteration, as a complete loss of phosphorylation induces PIN1:GFP intracellular accumulation (Figures 6D and 6E). This mislocalized PIN1:GFP S1,2,3A interfered with auxin accumulation (Figures 6G and 6H), resulting in strong embryo defects (Figure 6B), similar to embryo defects of *gnom* and *pp2aa1,3* loss-of-function (Mayer et al., 1993; Michniewicz et al., 2007) or *PID* gain-of-function (*RPS5A>>PID*) (Friml et al., 2004) mutants. The common reason for the embryo defects in these different mutants is that the basal localization of PIN1 in the provascular cells is lost, disturbing auxin accumulation in the basal tier of the embryo (Steinmann et al., 1999; Friml et al., 2004; Michniewicz et al., 2007; Figures 6G and 6H), which leads to auxin-regulated embryo defects. The enhanced intracellular accumulation of loss-of-phosphorylation PIN1 (PIN1:GFP S1,2,3A) is in line with the observation of PIN2 accumulation in endomembrane structures in *pid-9* loss-of-function mutant roots (Sukumar et al., 2009), which suggests that low levels of PID activity result in intracellular accumulation of PIN proteins. Loss-of-phosphorylation-induced intracellular PIN1 accumulation might be a result of reduced recycling to the PM, increased endocytosis, or reduced sorting from endosomes to the vacuoles. Further research is needed to distinguish between these possibilities.

AGC Kinases and PIN Proteins: A Stable Marriage in Plant Evolution

PID belongs to the plant-specific AGCVIII family of protein kinases, which are plant orthologs of the mammalian cAMP-dependent PKA, cGMP-dependent protein kinase G, and protein kinase C (Bögre et al., 2003). Among the three identified Ser residues, two (S2 and S3) are recognized by NetPhos as PKA phosphorylation targets (Blom et al., 1999), corroborating previous suggestions that the plant AGCVIII kinases might have been derived from the same ancestral kinase as animal PKAs (Bögre et al., 2003; Galván-Ampudia and Offringa, 2007).

In *Arabidopsis*, PID groups together with 22 other AGCVIII protein kinases (Bögre et al., 2003; Galván-Ampudia and Offringa, 2007), of which the blue light receptors PHOT1 and PHOT2, the root growth regulators WAG1 and WAG2, and the D6 protein kinases (D6PKs) have also been shown to be involved in auxin transport-regulated plant development (Sakai et al., 2001; Santner and Watson, 2006; Zourelidou et al., 2009). Previously, it was shown that the PIN1HL is also phosphorylated by D6PKs (Zourelidou et al., 2009). Although the D6PK genes showed a genetic interaction with *PIN1*, the D6PK protein had no effect on PIN1 polarity regulation (Friml et al., 2004; Michniewicz et al., 2007; Zourelidou et al., 2009). Further investigation into the possible D6PK phosphorylation targets in PINs should provide insight into the differential action of the distinct regulatory pathways by PID and D6PKs. PID, together with WAG1, WAG2, and AGC3-4, groups to the AGC3 clade within the AGCVIII family (Galván-Ampudia and Offringa, 2007). The localization of all four kinases at the plasma membrane (Galván-Ampudia and Offringa, 2007), and their genetic interactions (Cheng et al., 2008), suggest functional redundancy among the AGC3 kinases. In our studies,

complete loss of phosphorylation leads to not only PID-related morphological and cellular defects, but also defects never observed in PID-regulated processes. This leads us to hypothesize that the three phosphoserines identified here are not only targets of PID, but also of other AGC3 kinases, and might explain why *pid* loss of function does not lead to apical-to-basal PIN2 polarity changes in the root (Sukumar et al., 2009) or why the strong embryo defects induced by *PIN1:GFP S1,2,3A* are not observed in *pid* mutants. Further research is needed to validate this hypothesis.

Our data, together with the conclusion that PIN proteins and PID-like kinases coevolved during the transition of plants from water to land (Galván-Ampudia and Offringa, 2007), as well as the demonstrated functional relationship between PID and PINs (Friml et al., 2004), lead us to propose that phosphorylation of the conserved Ser residues plays an important role in PIN-dependent auxin transport throughout the evolution of plants. However, many questions still need to be answered. Functional analysis concerning phosphorylation of the three Ser residues in other PIN proteins and the regulation of PIN proteins by other AGC kinases will be the next challenges for the coming years.

METHODS

Plant Material, Growth Conditions, and Phenotypic Analysis

For all experiments, *Arabidopsis thaliana* of ecotype Col-0 was used. Construction of *PIN1:GFP* (to produce PIN1:GFP fusion proteins) and *P35S:PID* (to overexpress PID) and the corresponding *Arabidopsis* lines were described previously (Benjamins et al., 2001; Benkova et al., 2003). The loss-of-function alleles *pid-14* (SALK_049736) and *pin1* (SALK_047613) were obtained from the Nottingham *Arabidopsis* Stock Centre.

Seedlings were grown on MA medium (Masson and Paszkowski, 1992) at 21°C and a 16-h-light/8-h-dark photoperiod. One-week-old seedlings were transferred to MA medium supplemented with 50 µM naphthalylphthalamic acid (Pfaltz and Bauer), an auxin transport inhibitor, to induce pin inflorescences. The number of seedlings with root meristem collapse was counted 4, 6, and 8 d after germination. Plants were grown on a mixture of 9:1 substrate soil and sand (Holland Potgrond) at 21°C, a 16-h photoperiod, and 70% relative humidity.

DNA Constructs, Sequence Alignment, and Plant Transformation

Molecular cloning, DNA sequence analysis, and DNA and protein sequence alignments were performed using the Vector NTI 10 software (Invitrogen). For the *in silico* prediction of putative phosphorylation sites, we used the NetPhos software (Blom et al., 1999). The *pET-PIN1HL* (Gälweiler et al., 1998) and *pGEX-PID* (Benjamins et al., 2003) constructs have been described before. The *pET-PID* fusion construct was generated by cloning the *PID* cDNA into the *pET16B* (Novagen) derivative *pET16H*, which was kindly provided by Johan Memelink. The *pGEX-PIN1HL* fusion was generated by cloning the *PIN1HL Sma*I/*Sall* fragment from *pACT2-PIN1HL* into the corresponding restriction sites of plasmid *pGEX-KG* (Guan and Dixon, 1991). For construct *pGreen0229 PPIN1:PIN1:GFP*, the *PIN1* gene was amplified from Col-0 DNA using primers *PIN1F* 5'-CGAATTCTTATTCCATTGGCGTTGTC-3' and *PIN1R* 5'-CAGGTACCCACTTCTTATTGGTGAGA-3', and the fragment was digested with *Eco*RI and *Kpn*I, and cloned into the corresponding sites of *pGreen0229*. Subsequently, the *Bst*API fragment in this genomic clone was exchanged for the *Bst*API fragment containing the *PIN1:GFP* translational fusion from *pBIN-PPIN1:PIN1:GFP* (Friml et al., 2003). The

Quickchange XL site-directed mutagenesis kit (Stratagene) was used to generate mutant constructs. Oligonucleotides used for mutagenesis are listed in Supplemental Table 1 online. *Arabidopsis* plants were transformed by the floral dip method as described (Clough and Bent, 1998).

Protein Purification and in Vitro Phosphorylation Assays

Protein purification and in vitro phosphorylation assays were performed as described before (Benjamins et al., 2003; Michniewicz et al., 2007), with the following specifications. GST/HIS-tagged full-length PID and different mutant versions of GST/HIS-tagged PIN1HL proteins were used in in vitro phosphorylation assays. Cultures of *Escherichia coli* strain Rosetta (Novagen) containing the constructs were grown at 37°C to OD₆₀₀ = 0.6 in 50 mL LC supplemented with 100 µg/mL carbenicillin, 30 µg/mL chloramphenicol, and 25 µg/mL kanamycin. The cultures were then induced for 4 h with 1 mM isopropyl β-D-1-thiogalactopyranoside at 30°C, after which cells were harvested by centrifugation (20 min at 4000 rpm, 4°C in tabletop centrifuge) and frozen in liquid nitrogen. Precipitated cells were resuspended in 2 mL extraction buffer (EB; 1× PBS, 2 mM EDTA, and 2 mM DTT, pH 8.0) supplemented with 0.1% Tween 20 and 0.1 mM of the protease inhibitors phenylmethanesulfonyl fluoride, leupeptin, and aprotinin (Sigma-Aldrich) and sonicated for 2 min on ice. From this point on, all steps were performed at 4°C. Eppendorf tubes containing the sonicated cells were centrifuged at full speed (14,000 rpm) for 20 min, and the supernatants were transferred to 15-mL tubes containing 100 µL preequilibrated glutathione sepharose resin from GE Healthcare (pre-equilibration performed with three washes of EB). Resin-containing mixtures were incubated with gentle agitation for 1 h, subsequently centrifuged at 500 relative centrifugal force for 3 min, and the precipitated resin was washed three times with 20 resin volumes of EB. Then, three resin volumes of glutathione elution buffer (10 mM reduced glutathione and 50 mM Tris-HCl, pH 8.0) were added to the glutathione sepharose resin, and the mixture was agitated for 10 min at room temperature with gentle agitation. The resin was subsequently centrifuged for 3 min at 500 RCF, and the supernatant containing the desired protein was transferred to a new tube; this process was repeated twice more. The solutions containing the proteins were diluted 1000-fold in Tris buffer (25 mM Tris-HCl, pH 7.5, and 1 mM DTT) and concentrated to a workable volume (usually 50 µL) using Vivaspin microconcentrators with a 10-kD cutoff and a maximum capacity of 600 µL (Vivascience). Glycerol was added as preservative to a final concentration of 10%, and samples were stored at -80°C.

Approximately 1 µg of each purified GST/HIS-tagged protein (PID and substrates) was added to a 20 µL kinase reaction mix, containing 1× kinase buffer (25 mM Tris-HCl, pH 7.5, 1 mM DTT, and 5 mM MgCl₂) and 1× labeled ATP solution (100 µM MgCl₂/ATP and 1 µCi [γ-³²P]ATP). Reactions were incubated at 30°C for 30 min and stopped by addition of 5 µL of 5× protein loading buffer (310 mM Tris-HCl, pH 6.8, 10% SDS, 50% glycerol, 750 mM β-mercaptoethanol, and 0.125% bromophenol blue) and boiling for 5 min. Reactions were subsequently separated over 10% acrylamide gels, which were washed three times for 30 min with Kinase Gel wash buffer (5% trichloroacetic acid and 1% Na₂H₂P₂O₇), stained with Coomassie Brilliant Blue, and dried. Autoradiography was performed for 24 to 48 h at -80°C using Fuji Super RX x-ray films and intensifier screens. The relative intensity of phosphorylation bands was analyzed using ImageJ software (<http://rsb.info.nih.gov/ij/>).

For the peptide assays, 1 µg of purified PID was incubated with 4 nmol of 9^{mer} biotinylated peptides (Pepscan) in a phosphorylation reaction as described above. Reaction processing, spotting, and washing of the SAM² Biotin Capture Membrane (Promega) were performed according to the protocol of the manufacturer. Following washing, the membranes were sealed in plastic wrap and exposed to x-ray films for 24 to 48 h at -80°C using intensifier screens. The phosphorylation intensities of the peptides were determined by densitometry analysis of the autoradiographs using the ImageQuant software (Molecular Dynamics).

Membrane Protein Extraction and Protein Gel Blot Analysis

For the protein gel blot analysis, shoots from 7-d-old seedlings (grown on 1% agar medium containing 0.5× Gamborg-B5 and 1% sucrose, with a 16-h-light/8-h-dark photoperiod) were used to extract the membrane protein fraction. For the PIN1:GFP S1,2,3A mutant, shoots from 3-week-old heterozygote seedlings selected on antibiotic plates were used. Membrane protein extraction and protein gel blot analyses were described recently (Abas and Luschnig, 2010).

Immunolocalization, Microscopy, and Signal Analysis

Whole-mount immunolocalization was performed as described (Friml et al., 2004), using rabbit anti-PIN2 (dilution 1:200; Abas et al., 2006) and rabbit anti-PIN4 (dilution 1:200; Friml et al., 2004) as the primary antibody and an anti-rabbit Alexa 488 conjugate as the secondary antibody (dilution 1:200; Molecular Probes).

PIN1:GFP signal in shoots and embryos and DR5:GFP signal in roots (used in Figures 7G to 7L) were visualized in water without fixation. PIN1:GFP signal in 3-d-old seedling roots (used in Figures 7A to 7F) was visualized with fixation and permeation steps as described (Friml et al., 2004). Signals were detected with confocal laser scanning microscopy (Zeiss LSM 5 confocal microscope). The images were processed by ImageJ software (<http://rsb.info.nih.gov/ij/>) and assembled in Adobe Photoshop CS2. PDR5:GFP signal intensity was measured by ImageJ, and error bars were obtained based on the measurement of three to six seedling roots per line. The Y value is the average DR5 signal intensity of each line relative to that in wild-type PIN1:GFP line.

Embryo development was analyzed by differential interference contrast microscopy (Zeiss Axioplan2) on cleared ovules (1-h treatment in the clearing solution of chloral hydrate:H₂O:glycerol = 8:3:1).

Accession Numbers

Sequence data from this article can be found in The Arabidopsis Information Resource (<http://www.Arabidopsis.org/>) or GenBank/EMBL databases under the following accession numbers: *Arabidopsis* PIN1 (gi:15219501), *Arabidopsis* PIN2 (gi:42558886), *Arabidopsis* PIN3 (gi:42558887), *Arabidopsis* PIN4 (gi:42558871), *Arabidopsis* PIN6 (gi:42558888), *Arabidopsis* PIN7 (gi:42558877), barrel medic (*Medicago truncatula*) PIN1 (gi:25986771), rice (*Oryza sativa*) PIN1 (gi:75251559), moss (*Physcomitrella patens*) PIN1 (gi:55859521), and maize (*Zea mays*) PIN1c (gi:171850415). *Arabidopsis* T-DNA insertion mutants representing the loss-of-function alleles are SALK_049736 (*pid-14*) and SALK_047613 (*pin1*). Nottingham Arabidopsis Stock Centre identification numbers for the transgenic *Arabidopsis* lines PIN1:GFP and P35S:PID are N9362 and N9867, respectively.

Supplemental Data

The following materials are available in the online version of this article.

Supplemental Figure 1. Amino Acid Sequence of the *Arabidopsis* PIN1 Protein.

Supplemental Figure 2. Relative in Vitro Phosphorylation Intensities of Peptides Containing Putative Phosphorylation Sites in the PIN1HL (Boxed) by PID.

Supplemental Figure 3. In Vitro Phosphorylation Assays of Predicted Phosphorylation Targets in the PIN1HL by PID.

Supplemental Figure 4. Alignment of the Amino Acid Sequences of the PIN1 Proteins from Five Plant Species Showing the Evolutionary Conservation of the Three TPRXS(N/S) Motifs.

Supplemental Figure 5. Quantification of Protein Expression by Western Blot Analysis Using PIN1-Specific Antibody.

Supplemental Figure 6. Confocal Laser Scanning Microscopy Images of Mutated PIN1:GFP Localization.

Supplemental Figure 7. Quantification of Auxin Reporter PDR5:GFP Expression in Root Tips.

Supplemental Table 1. Oligonucleotides Used in Site-Directed Mutagenesis.

ACKNOWLEDGMENTS

We thank G. Lamers for technical help with confocal laser scanning microscopy, D. Doevedans for making construct *pGreen0229 PPIN1:PIN1:GFP*, S. Peck and A. Jones for providing unpublished information on mass spectrometry-detected *in vivo* phosphoresidues in the PINHL, K. Palme for kindly providing the yeast two-hybrid plasmid *pACT2-PIN1HL*, and A. Vivian-Smith and K. Boutiller for their helpful comments on an earlier version of the manuscript. This work was supported by grants from the China Scholarship Council (F.H.), from the Brazilian Funding Agency for Post-Graduation Education-Coordenação de Aperfeiçoamento de Pessoal de Nível Superior (M.K.-Z.), from the Austrian Science Fund FWF project P21533 (L.A.), from the Research Council for Earth and Life Sciences (C.S.G.-A., ALW 813.06.004 to R.O.), and from the Research Council for Chemical Sciences (F.H., CW 700.58.301 to R.O.) with financial aid from The Netherlands Organization for Scientific Research.

Received November 11, 2009; revised March 1, 2010; accepted March 27, 2010; published April 20, 2010.

REFERENCES

Abas, L., Benjamins, R., Malenica, N., Paciorek, T., Wiśniewska, J., Moulinier-Anzola, J.C., Sieberer, T., Friml, J., and Luschnig, C. (2006). Intracellular trafficking and proteolysis of the *Arabidopsis* auxin-efflux facilitator PIN2 are involved in root gravitropism. *Nat. Cell Biol.* **8**: 249–256.

Abas, L., and Luschnig, C. (March 1, 2010). Maximum yields of microsomal-type membranes from small amounts of plant material without requiring ultracentrifugation. *Anal. Biochem.* <http://dx.doi.org/10.1016/j.ab.2010.02.030>.

Benjamins, R., Galván-Ampudia, C.S., Hooykaas, P.J., and Offringa, R. (2003). PINOID-mediated signaling involves calcium-binding proteins. *Plant Physiol.* **132**: 1623–1630.

Benjamins, R., Quint, A., Weijers, D., Hooykaas, P., and Offringa, R. (2001). The PINOID protein kinase regulates organ development in *Arabidopsis* by enhancing polar auxin transport. *Development* **128**: 4057–4067.

Benkova, E., Michniewicz, M., Sauer, M., Teichmann, T., Seifertová, D., Jürgens, G., and Friml, J. (2003). Local, efflux-dependent auxin gradients as a common module for plant organ formation. *Cell* **115**: 591–602.

Bennett, S.R.M., Alvarez, J., Bossinger, G., and Smyth, D.R. (1995). Morphogenesis in *pinoid* mutants of *Arabidopsis thaliana*. *Plant J.* **8**: 505–520.

Benschop, J.J., Mohammed, S., O'Flaherty, M., Heck, A.J., Slijper, M., and Menke, F.L. (2007). Quantitative phosphoproteomics of early elicitor signaling in *Arabidopsis*. *Mol. Cell. Proteomics* **6**: 1198–1214.

Blilou, I., Xu, J., Wildwater, M., Willemsen, V., Paponov, I., Friml, J., Heidstra, R., Aida, M., Palme, K., and Scheres, B. (2005). The PIN auxin efflux facilitator network controls growth and patterning in *Arabidopsis* roots. *Nature* **433**: 39–44.

Blom, N., Gammeltoft, S., and Brunak, S. (1999). Sequence and structure-based prediction of eukaryotic protein phosphorylation sites. *J. Mol. Biol.* **294**: 1351–1362.

Bögre, L., Ökrész, L., Henriques, R., and Anthony, R.G. (2003). Growth signalling pathways in *Arabidopsis* and the AGC protein kinases. *Trends Plant Sci.* **8**: 424–431.

Carraro, N., Forestan, C., Canova, S., Traas, J., and Varotto, S. (2006). *ZmPIN1a* and *ZmPIN1b* encode two novel putative candidates for polar auxin transport and plant architecture determination of maize. *Plant Physiol.* **142**: 254–264.

Casanova, J.E., Breitfeld, P.P., Ross, S.A., and Mostov, K.E. (1990). Phosphorylation of the polymeric immunoglobulin receptor required for its efficient transcytosis. *Science* **248**: 742–745.

Cheng, Y., Qin, G., Dai, X., and Zhao, Y. (2008). NPY genes and AGC kinases define two key steps in auxin-mediated organogenesis in *Arabidopsis*. *Proc. Natl. Acad. Sci. USA* **105**: 21017–21022.

Christensen, S.K., Dagenais, N., Chory, J., and Weigel, D. (2000). Regulation of auxin response by the protein kinase PINOID. *Cell* **100**: 469–478.

Clough, S.J., and Bent, A.F. (1998). Floral dip: A simplified method for *Agrobacterium*-mediated transformation of *Arabidopsis thaliana*. *Plant J.* **16**: 735–743.

Delbarre, A., Muller, P., and Guern, J. (1998). Short-lived and phosphorylated proteins contribute to carrier-mediated efflux, but not to influx, of auxin in suspension-cultured tobacco cells. *Plant Physiol.* **116**: 833–844.

Dhonukshe, P., et al. (2008). Generation of cell polarity in plants links endocytosis, auxin distribution and cell fate decisions. *Nature* **456**: 962–966.

Friml, J., Benková, E., Blilou, I., Wisniewska, J., Hamann, T., Ljung, K., Woody, S., Sandberg, G., Scheres, B., Jürgens, G., and Palme, K. (2002a). AtPIN4 mediates sink-driven auxin gradients and root patterning in *Arabidopsis*. *Cell* **108**: 661–673.

Friml, J., Vieten, A., Sauer, M., Weijers, D., Schwarz, H., Hamann, T., Offringa, R., and Jürgens, G. (2003). Efflux-dependent auxin gradients establish the apical-basal axis of *Arabidopsis*. *Nature* **426**: 147–153.

Friml, J., Wiśniewska, J., Benková, E., Mendgen, K., and Palme, K. (2002b). Lateral relocation of auxin efflux regulator PIN3 mediates tropism in *Arabidopsis*. *Nature* **415**: 806–809.

Friml, J., et al. (2004). A PINOID-dependent binary switch in apical-basal PIN polar targeting directs auxin efflux. *Science* **306**: 862–865.

Furutani, M., Vernoux, T., Traas, J., Kato, T., Tasaka, M., and Aida, M. (2004). PIN-FORMED1 and PINOID regulate boundary formation and cotyledon development in *Arabidopsis* embryogenesis. *Development* **131**: 5021–5030.

Galván-Ampudia, C.S., and Offringa, R. (2007). Plant evolution: AGC kinases tell the auxin tale. *Trends Plant Sci.* **12**: 541–547.

Gälweiler, L., Guan, C., Müller, A., Wisman, E., Mendgen, K., Yephremov, A., and Palme, K. (1998). Regulation of polar auxin transport by AtPIN1 in *Arabidopsis* vascular tissue. *Science* **282**: 2226–2230.

Garbers, C., DeLong, A., Deruère, J., Bernasconi, P., and Söll, D. (1996). A mutation in protein phosphatase 2A regulatory subunit A affects auxin transport in *Arabidopsis*. *EMBO J.* **15**: 2115–2124.

Geisler, M., and Murphy, A.S. (2006). The ABC of auxin transport: The role of p-glycoproteins in plant development. *FEBS Lett.* **580**: 1094–1102.

Geldner, N., Anders, N., Wolters, H., Keicher, J., Kornberger, W., Müller, P., Delbarre, A., Ueda, T., Nakano, A., and Jürgens, G. (2003). The *Arabidopsis* GNOM ARF-GEF mediates endosomal recycling, auxin transport, and auxin-dependent plant growth. *Cell* **112**: 219–230.

Geldner, N., Friml, J., Stierhof, Y.-D., Jürgens, G., and Palme, K. (2001). Auxin transport inhibitors block PIN1 cycling and vesicle trafficking. *Nature* **413**: 425–428.

Guan, K.L., and Dixon, J.E. (1991). Eukaryotic proteins expressed in *Escherichia coli*: An improved thrombin cleavage and purification procedure of fusion proteins with glutathione S-transferase. *Anal. Biochem.* **192**: 262–267.

Harrison, B.R., and Masson, P.H. (2008). ARL2, ARG1 and PIN3 define a gravity signal transduction pathway in root statocytes. *Plant J.* **53**: 380–392.

Heisler, M.G., Ohno, C., Das, P., Sieber, P., Reddy, G.V., Long, J.A., and Meyerowitz, E.M. (2005). Patterns of auxin transport and gene expression during primordium development revealed by live imaging of the *Arabidopsis* inflorescence meristem. *Curr. Biol.* **15**: 1899–1911.

Kleine-Vehn, J., Dhonukshe, P., Sauer, M., Brewer, P.B., Wiśniewska, J., Paciorek, T., Benková, E., and Friml, J. (2008). ARF GEF-dependent transcytosis and polar delivery of PIN auxin carriers in *Arabidopsis*. *Curr. Biol.* **18**: 526–531.

Kleine-Vehn, J., Huang, F., Naramoto, S., Zhang, J., Michniewicz, M., Offringa, R., and Friml, J. (2009). PIN auxin efflux carrier polarity is regulated by PINOID kinase-mediated recruitment into GNOM-independent trafficking in *Arabidopsis*. *Plant Cell* **21**: 3839–3849.

Liu, Y., and Zhang, S. (2004). Phosphorylation of 1-aminocyclopropane-1-carboxylic acid synthase by MPK6, a stress-responsive mitogen-activated protein kinase, induces ethylene biosynthesis in *Arabidopsis*. *Plant Cell* **16**: 3386–3399.

Masson, J., and Paszkowski, J. (1992). The culture response of *Arabidopsis thaliana* protoplasts is determined by the growth-conditions of donor plants. *Plant J.* **2**: 829–833.

Mayer, U., Büttner, G., and Jürgens, G. (1993). Apical-basal pattern-formation in the *Arabidopsis* embryo - Studies on the role of the *gnom* gene. *Development* **117**: 149–162.

McSteen, P., Malcomber, S., Skirpan, A., Lunde, C., Wu, X., Kellogg, E., and Hake, S. (2007). *barren inflorescence2* encodes a co-ortholog of the PINOID serine/threonine kinase and is required for organogenesis during inflorescence and vegetative development in maize. *Plant Physiol.* **144**: 1000–1011.

Michniewicz, M., et al. (2007). Antagonistic regulation of PIN phosphorylation by PP2A and PINOID directs auxin flux. *Cell* **130**: 1044–1056.

Morita, Y., and Kyozuka, J. (2007). Characterization of OsPID, the rice ortholog of PINOID, and its possible involvement in the control of polar auxin transport. *Plant Cell Physiol.* **48**: 540–549.

Mravec, J., et al. (2009). Subcellular homeostasis of phytohormone auxin is mediated by the ER-localized PIN5 transporter. *Nature* **459**: 1136–1140.

Müller, A., Guan, C., Gälweiler, L., Tänzler, P., Huijser, P., Marchant, A., Parry, G., Bennett, M., Wisman, E., and Palme, K. (1998). *AtPIN2* defines a locus of *Arabidopsis* for root gravitropism control. *EMBO J.* **17**: 6903–6911.

Nühse, T.S., Stensballe, A., Jensen, O.N., and Peck, S.C. (2004). Phosphoproteomics of the *Arabidopsis* plasma membrane and a new phosphorylation site database. *Plant Cell* **16**: 2394–2405.

Okada, K., Ueda, J., Komaki, M.K., Bell, C.J., and Shimura, Y. (1991). Requirement of the auxin polar transport system in early stages of *Arabidopsis* floral bud formation. *Plant Cell* **3**: 677–684.

Paciorek, T., Zažímalová, E., Ruthardt, N., Petrášek, J., Stierhof, Y.-D., Kleine-Vehn, J., Morris, D.A., Emans, N., Jürgens, G., Geldner, N., and Friml, J. (2005). Auxin inhibits endocytosis and promotes its own efflux from cells. *Nature* **435**: 1251–1256.

Paponov, I.A., Teale, W.D., Trebar, M., Blilou, I., and Palme, K. (2005). The PIN auxin efflux facilitators: evolutionary and functional perspectives. *Trends Plant Sci.* **10**: 170–177.

Parry, G., et al. (2001). Quick on the uptake: Characterization of a family of plant auxin influx carriers. *J. Plant Growth Regul.* **20**: 217–225.

Pearson, G., Robinson, F., Beers, G.T., Xu, B.E., Karandikar, M., Berman, K., and Cobb, M.H. (2001). Mitogen-activated protein (MAP) kinase pathways: Regulation and physiological functions. *Endocr. Rev.* **22**: 153–183.

Rashotte, A.M., DeLong, A., and Muday, G.K. (2001). Genetic and chemical reductions in protein phosphatase activity alter auxin transport, gravity response, and lateral root growth. *Plant Cell* **13**: 1683–1697.

Reinhardt, D., Pesce, E.R., Stieger, P., Mandel, T., Baltensperger, K., Bennett, M., Traas, J., Friml, J., and Kuhlemeier, C. (2003). Regulation of phyllotaxis by polar auxin transport. *Nature* **426**: 255–260.

Sabatini, S., Beis, D., Wolkenfels, H., Murfett, J., Guilfoyle, T., Malamy, J., Benfey, P., Leyser, O., Bechtold, N., Weisbeek, P., and Scheres, B. (1999). An auxin-dependent distal organizer of pattern and polarity in the *Arabidopsis* root. *Cell* **99**: 463–472.

Sakai, T., Kagawa, T., Kasahara, M., Swartz, T.E., Christie, J.M., Briggs, W.R., Wada, M., and Okada, K. (2001). *Arabidopsis nph1* and *npl1*: Blue light receptors that mediate both phototropism and chloroplast relocation. *Proc. Natl. Acad. Sci. USA* **98**: 6969–6974.

Santner, A.A., and Watson, J.C. (2006). The WAG1 and WAG2 protein kinases negatively regulate root waving in *Arabidopsis*. *Plant J.* **45**: 752–764.

Sauer, M., Balla, J., Luschnig, C., Wiśniewska, J., Reinöhl, V., Friml, J., and Benková, E. (2006). Canalization of auxin flow by Aux/IAA-ARF-dependent feedback regulation of PIN polarity. *Genes Dev.* **20**: 2902–2911.

Skirpan, A., Culler, A.H., Gallavotti, A., Jackson, D., Cohen, J.D., and McSteen, P. (2009). BARREN INFLORESCENCE2 interaction with ZmPIN1a suggests a role in auxin transport during maize inflorescence development. *Plant Cell Physiol.* **50**: 652–657.

Sorefan, K., Girin, T., Liljegren, S.J., Ljung, K., Robles, P., Galván-Ampudia, C.S., Offringa, R., Friml, J., Yanofsky, M.F., and Østergaard, L. (2009). A regulated auxin minimum is required for seed dispersal in *Arabidopsis*. *Nature* **459**: 583–586.

Steinmann, T., Geldner, N., Grebe, M., Mangold, S., Jackson, C.L., Paris, S., Gälweiler, L., Palme, K., and Jürgens, G. (1999). Coordinated polar localization of auxin efflux carrier PIN1 by GNOM ARF GEF. *Science* **286**: 316–318.

Sukumar, P., Edwards, K.S., Rahman, A., Delong, A., and Muday, G.K. (2009). PINOID kinase regulates root gravitropism through modulation of PIN2-dependent basipetal auxin transport in *Arabidopsis thaliana*. *Plant Physiol.* **150**: 722–735.

Viéte, A., Vanneste, S., Wiśniewska, J., Benková, E., Benjamins, R., Beeckman, T., Luschnig, C., and Friml, J. (2005). Functional redundancy of PIN proteins is accompanied by auxin-dependent cross-regulation of PIN expression. *Development* **132**: 4521–4531.

Wiśniewska, J., Xu, J., Seifertová, D., Brewer, P.B., Růžička, K., Blilou, I., Rouquié, D., Benková, E., Scheres, B., and Friml, J. (2006). Polar PIN localization directs auxin flow in plants. *Science* **312**: 883.

Xu, M., Zhu, L., Shou, H., and Wu, P. (2005). A *PIN1* family gene, *OsPIN1*, involved in auxin-dependent adventitious root emergence and tillering in rice. *Plant Cell Physiol.* **46**: 1674–1681.

Zhang, J., Nodzyński, T., Pěnčík, A., Rolčík, J., and Friml, J. (2010). PIN phosphorylation is sufficient to mediate PIN polarity and direct auxin transport. *Proc. Natl. Acad. Sci. USA* **107**: 918–922.

Zourelidou, M., Müller, I., Willige, B.C., Nill, C., Jikumaru, Y., Li, H., and Schwechheimer, C. (2009). The polarly localized D6 PROTEIN KINASE is required for efficient auxin transport in *Arabidopsis thaliana*. *Development* **136**: 627–636.

Phosphorylation of Conserved PIN Motifs Directs *Arabidopsis* PIN1 Polarity and Auxin Transport

Fang Huang, Marcelo Kemel Zago, Lindy Abas, Arnoud van Marion, Carlos Samuel Galván-Ampudia and Remko Offringa

Plant Cell 2010;22:1129-1142; originally published online April 20, 2010;
DOI 10.1105/tpc.109.072678

This information is current as of November 1, 2017

Supplemental Data	/content/suppl/2010/04/06/tpc.109.072678.DC1.html
References	This article cites 61 articles, 26 of which can be accessed free at: /content/22/4/1129.full.html#ref-list-1
Permissions	https://www.copyright.com/ccc/openurl.do?sid=pd_hw1532298X&issn=1532298X&WT.mc_id=pd_hw1532298X
eTOCs	Sign up for eTOCs at: http://www.plantcell.org/cgi/alerts/ctmain
CiteTrack Alerts	Sign up for CiteTrack Alerts at: http://www.plantcell.org/cgi/alerts/ctmain
Subscription Information	Subscription Information for <i>The Plant Cell</i> and <i>Plant Physiology</i> is available at: http://www.aspб.org/publications/subscriptions.cfm